# The vertical transport of methane from different potential emission types on Mars

AGU PUBLICATIONS

Geophysical Research Letters

RESEARCH LETTER
10.1002/2017GL074613

**Key Points:**
- Determining if a methane surface source is a sustained or instantaneous release requires 10 sols of tracking the emission
- An instantaneous surface or atmosphere methane release is indistinguishable after around 5 sols of emission
- Assimilation of thermal data are critical for the correct backtracking of a methane source to its origin

**Supporting Information:**
- Supporting Information S1

**Correspondence to:**
J. A. Holmes,
james.holmes@open.ac.uk

**Citation:**
Holmes, J. A., M. R. Patel, and S. R. Lewis (2017), The vertical transport of methane from different potential emission types on Mars, *Geophys. Res. Lett.*, *44*, 8611–8620, doi:10.1002/2017GL074613.

Received 18 JUN 2017
Accepted 6 AUG 2017
Accepted article online 14 AUG 2017
Published online 26 AUG 2017



# The vertical transport of methane from different potential emission types on Mars

**J. A. Holmes**[1], **M. R. Patel**[1,2], **and S. R. Lewis**[1]

[1]School of Physical Sciences, Open University, Milton Keynes, UK, [2]Space Science and Technology Department, Science and Technology Facilities Council, Rutherford Appleton Laboratory, Didcot, UK

**Abstract** The contrasting evolutionary behavior of the vertical profile of methane from three potential release scenarios is analyzed using a global circulation model with assimilated temperature profiles. Understanding the evolving methane distribution is essential for interpretation of future retrievals of the methane vertical profile taken by instruments on the ExoMars Trace Gas Orbiter spacecraft. We show that at methane release rates constrained by previous observations and modeling studies, discriminating whether the methane source is a sustained or instantaneous surface emission requires at least 10 sols of tracking the emission. A methane source must also be observed within 5 to 10 sols of the initial emission to distinguish whether the emission occurs directly at the surface or within the atmosphere via destabilization of metastable clathrates. Assimilation of thermal data is shown to be critical for the most accurate backtracking of an observed methane plume to its origin.

## 1. Introduction

The existence of methane on Mars has recently been confirmed with an in situ detection by the NASA Curiosity rover [*Webster et al.*, 2015]. Recent modeling studies of methane surface release have shown that methane can form layers in the atmosphere [*Viscardy et al.*, 2016] and that surface releases of methane could potentially reconcile past observations from multiple different instruments [*Holmes et al.*, 2015]. The fact that a surface release of methane can evolve into a distinct atmospheric layer suggests that the local observations by the NASA Curiosity rover and past column observations by other instruments [*Mumma et al.*, 2009; *Fonti and Marzo*, 2010; *Geminale et al.*, 2011; *Villanueva et al.*, 2013] can potentially be reconcilable.

Multiple origins of methane on Mars have been hypothesized in the recent past, ranging from biogenesis [*Summers et al.*, 2002] to serpentinization [*Oze and Sharma*, 2005; *Atreya et al.*, 2007] and destabilization of methane clathrate hydrates [*Chassefière*, 2009]. By modeling transport of methane through the subsurface, *Stevens et al.* [2017] suggest that deep subsurface releases are not capable of providing the nonuniform sources of methane observed and that (if subsurface in origin) it must be as a result of fracturing or convective plumes from shallow sources. They also highlight that it is crucial to take into account transport processes when attempting to identify the source of any methane observed by future missions.

Future trace gas observations by the Nadir and Occultation for Mars Discovery (NOMAD) and Atmospheric Chemistry Suite (ACS) instruments on the ExoMars Trace Gas Orbiter (TGO) spacecraft will be the first to provide vertical profiles of methane, among multiple other species. For interpretation and understanding of the retrieved methane vertical profiles, modeling studies are required to scrutinize between the different proposed mechanisms of methane release into the atmosphere, with global circulations models (GCMs) providing an invaluable tool to investigate the evolution of trace gas plumes and provide knowledge on where the original source could be located, and also potentially clues to its origin.

Previous modeling studies investigating the evolution of a methane source have been limited by the use of modeled wind fields [*Lefèvre and Forget*, 2009; *Viscardy et al.*, 2016]. For the methane emission scenarios in this study, temperature retrievals from the Thermal Emission Spectrometer (TES) are assimilated using a modified form of the Analysis Correction (AC) scheme [*Lewis et al.*, 2007]. Since there are no direct global wind observations, and the assimilation scheme ensures the wind fields are consistent with the thermal data input to the model, the assimilation process results in the best constraint available on the transport of tracers in the Martian atmosphere and the best possible dynamical state of the atmosphere, of great importance

when attempting to backtrack the methane sources to their source location. It was also shown by *Lewis et al.* [2007] that actual transient wave behavior seen in observations is captured by the model when assimilating TES temperature profiles, rather than simply modifying the thermal state of the model to produce transient modes of different strengths and locations.

This study investigates the vertical evolution of methane from multiple different source emission scenarios, using a state-of-the-art Mars GCM coupled to the AC assimilation scheme. Section 2 details the GCM and observational data used in this investigation, with the evolving methane vertical profile from three different source emission scenarios analyzed in section 3. Finally, the difference in the evolution of the vertical profile of methane with/without the assimilation of thermal data is detailed in section 4.

## 2. Methods

This section details the GCM and observational data used to construct the simulations, followed by a description of the different emission scenarios investigated in this study.

### 2.1. Model and Observational Data

The Mars GCM used for this investigation is the UK version of the LMD GCM [*Forget et al.*, 1999], hereafter MGCM, which has been developed in a collaboration between the Laboratoire de Météorologie Dynamique, the Open University, the University of Oxford, and the Instituto de Astrofisica de Andalucia. This model uses physical parameterizations shared with the LMD GCM, which are coupled to a spectral dynamical core and semi-Lagrangian advection scheme [*Newman et al.*, 2002] to transport tracers. Tracers such as methane are transported by the semi-Lagrangian advection scheme with mass conservation [*Priestley*, 1993]. The advection scheme uses wind fields updated by the dynamical core to determine the methane concentration at each model grid point every 15 min.

The MGCM is similar to the model used in *Holmes et al.* [2015] but now includes additional submodels to improve on modeling of the planetary boundary layer and water and dust cycles. A thermal plume model is used to better represent turbulent structures in the planetary boundary layer [*Colaïtis et al.*, 2013], of critical importance for the evolution of tracers (e.g., methane) released from the surface. Regarding the Martian water cycle, the most recent cloud microphysics package is now included [*Navarro et al.*, 2014] which also accounts for the effects of radiatively active water ice clouds. A "semi-interactive" two-moment scheme is used to freely transport dust in the model [*Madeleine et al.*, 2011], although the dust column optical depth at each grid point is scaled to match the observed dust distribution maps created by *Montabone et al.* [2015] using an interpolation of numerous sets of observations from orbiters and landers based on a kriging method. The model is truncated at wave number 31 resulting in a 5° longitude-latitude grid with 35 vertical levels extending to an altitude of ~105 km (full details of the vertical levels used in this study are supplied in supporting information S1).

### 2.2. Simulations

Three different methane emission scenarios were used to investigate the evolutionary behavior of the methane vertical profile from an initial source. The area and timing of the methane release was chosen to coincide with the observed methane plume in 2003 by *Mumma et al.* [2009], using the closest GCM grid point located at 50°E, 2.5°N. Two different release methods are chosen, with either sustained emission over a 30 sol period starting at $L_S = 148°$ in MY 26 or an instantaneous emission in which methane is released over a single 15 min (one physics time step) time window. The release rate for the sustained emission scenario is constrained by the optimal scenario in *Lefèvre and Forget* [2009] for the development of the plume observed by *Mumma et al.* [2009], in which 150,000 t of methane is released over a 120 sol period. The resulting release rate, equivalent to continuous emission of methane at a rate of $3.3 \times 10^{-10}$ kg m$^{-2}$ s$^{-1}$ at the surface over the 30 sol period, is of similar magnitude to the best fit release rate estimated by *Holmes et al.* [2015] when attempting to reconcile the evolution of the observed plume [*Mumma et al.*, 2009] with observations later in time from a separate instrument [*Fonti and Marzo*, 2010].

Two separate simulations are performed for the instantaneous emission scenario. The release rate of methane in both simulations is constrained by the estimated observed plume mass of 19,000 t [*Mumma et al.*, 2009]. The first instantaneous emission scenario emits methane from the surface at 50°E, 2.5°N on the first model time step and then allows for the methane distribution to only be altered by transport processes. Comparison of the methane vertical distribution between the sustained and instantaneous surface emission

scenario could potentially be used to highlight any expected differences based on the different method of release. A third simulation also uses the instantaneous emission scenario, but the methane is released into the atmosphere at an altitude of 10 km instead of from the surface. In the case of destabilization of methane clathrate hydrates being the source of methane, the release could potentially be atmospheric rather than from the surface [*Chassefière*, 2009]. This process suggests that methane is transported into the atmosphere from the subsurface in a metastable clathrate form and decomposes into gaseous methane through the condensation-sublimation process of water vapor. At the time and latitude of the modeled methane release, water vapor is primarily confined to altitudes below 10 km [*Steele et al.*, 2014]. Comparison of the methane vertical profile in the instantaneous surface and atmosphere emission scenarios could potentially be used to highlight if it is possible to determine whether the atmospheric methane present originated from an initial surface/atmospheric source.

Temperature profiles from the Thermal Emission Spectrometer (TES) instrument [*Conrath et al.*, 2000] on the Mars Global Surveyor spacecraft are assimilated in all three different release scenarios to provide the most realistic thermodynamical state of the atmosphere, with almost one million temperature profiles assimilated over the 30 sol period of each simulation. The TES temperature profiles cover from the surface to an altitude of ~40 km, encompass all latitudes and are spaced by ~30° in longitude. One final simulation identical to the instantaneous surface emission scenario except without any data assimilation is included in section 4 to identify how the addition of thermal profiles by the assimilation process alters the distribution of the evolving methane plume.

## 3. Contrasting Evolution of Methane Vertical Profile

The horizontal movement of a methane source emission was detailed in *Holmes et al.* [2015] by analyzing the vertically integrated zonal and meridional flux of methane, while here we investigate and compare the evolution of the methane concentration from three different emission scenarios as a function of height in the atmosphere. This approach is taken as it represents the way in which these measurements will be made in future by the ExoMars TGO mission.

The evolution of the methane volume mixing ratio vertical profile at a latitude of 2.5°N (i.e., the latitude of the initial source emission) for the three different emission scenarios is shown in Figure 1. After 1 sol, the sustained and instantaneous surface emission scenario, shown in Figures 1a and 1b, respectively, are similarly transported, with only a difference in the amount transported as a result of the increased mass of methane added to the atmosphere in the instantaneous surface emission. Methane emitted from the surface source is predominantly transported by weak near-surface easterlies to around 30°E, while the local circulation patterns result in a portion of methane greater than 10 ppbv (parts per billion by volume) reaching altitudes beyond 10 km.

The longitudinal transport of methane in the instantaneous atmosphere emission scenario (Figure 1c) is likely to be more extensive as the zonal winds at an altitude of 10 km (the altitude of the atmospheric source emission) and higher are marginally stronger than near-surface winds. The complex nature of local circulation patterns as a result of turbulent structures in the planetary boundary layer results in methane at a level of ~1 ppbv reaching the surface at longitudes close to the initial longitude of the source (50°E).

As expected from a sustained or instantaneous surface source emission, after 1 sol peak amounts of methane greater than 10 ppbv are seen closest to the surface with methane decreasing at increasing altitude, whereas the instantaneous atmosphere emission scenario displays a peak in methane abundance centered at around 11 km altitude. After only 2 sols, the methane vertical profile directly over the initial source location in the instantaneous surface emission scenario (Figure 1e) has changed drastically, with a methane abundance greater than 10 ppbv centered at ~10 km altitude and less than 5 pptv (parts per trillion by volume) near the surface as a result of consistent westward transport of methane near the surface at this latitude. The sustained surface emission scenario after 2 sols, shown in Figure 1d, still has a large methane abundance near the surface (as a result of continued emission in this scenario) which is at least 2 orders of magnitudes larger than in the instantaneous surface emission scenario. Comparison of the methane vertical profile 20° westward of the initial source longitude, however, would indicate little difference between the sustained and instantaneous surface emission scenario except in the peak methane abundance resulting from the stronger initial release in the instantaneous surface emission scenario.

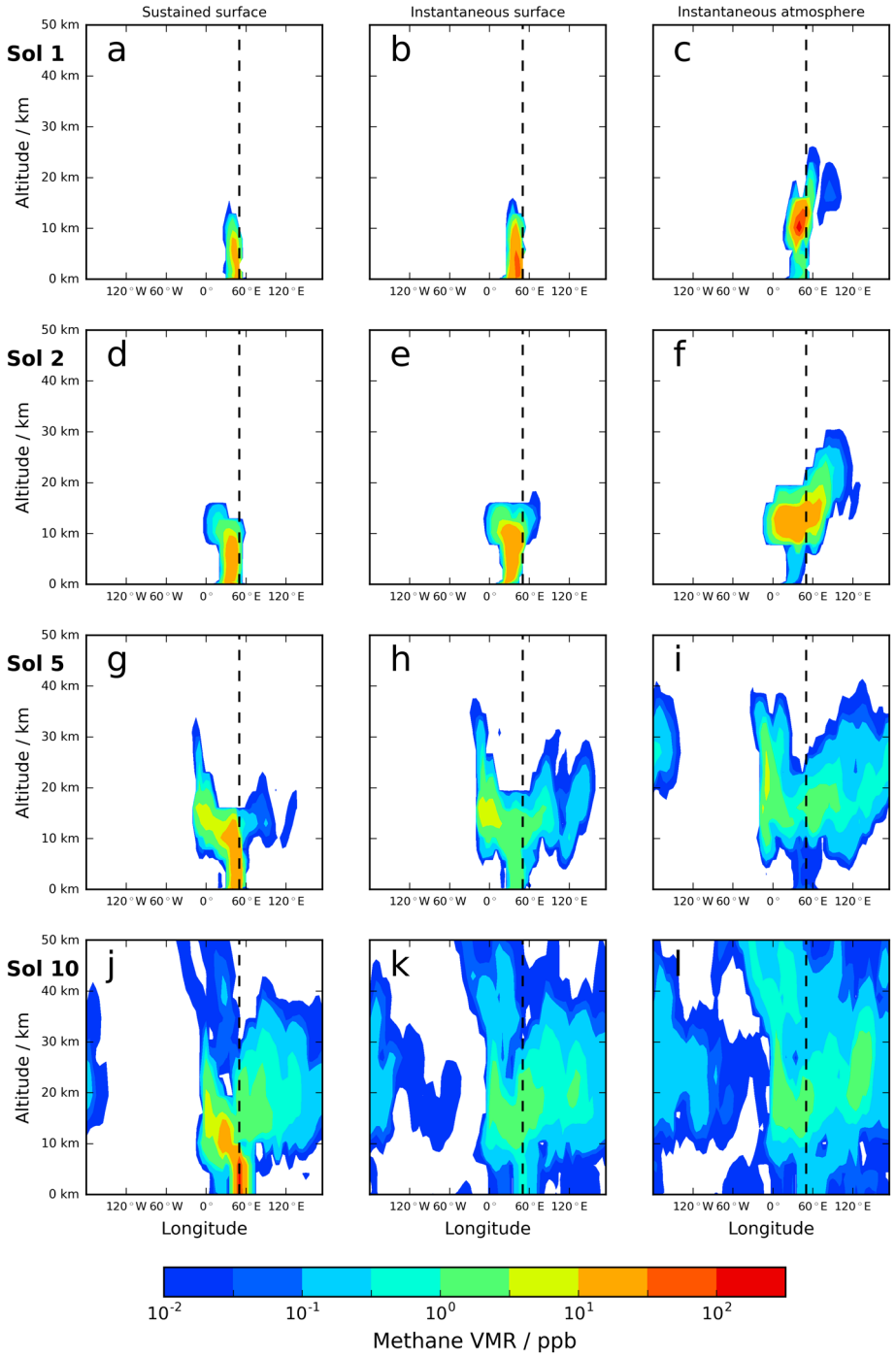


**Figure 1.** Meridional cross section of methane vertical profile at 2.5°N in the sustained surface release scenario (Figures 1a, 1d, 1g, and 1j), instantaneous surface release scenario (Figures 1b, 1e, 1h, and 1k), and instantaneous atmosphere release scenario (Figures 1c, 1f, 1i, and 1l) for the (a–c) first, (d–f) second, (g–i) fifth, and (j–l) tenth sol of simulation. The dashed vertical black line indicates the longitude of the initial source emission (50°E,2.5°N). White indicates methane at levels lower than 10 pptv.

Over the initial source location (50°E,2.5°N) after 2 sols, the methane vertical profile in the instantaneous atmosphere emission scenario (Figure 1f) is similar to the instantaneous surface emission scenario (Figure 1e) except for a slight difference in the center of the atmospheric layer (15 km in the instantaneous atmosphere emission scenario as opposed to 10 km). It is only by knowing the vertical profile of methane westward of the initial source longitude that we could distinguish between the surface or atmospheric

origin of methane, suggesting frequent spatial mapping of methane vertical profiles in longitudinal space are necessary.

The longitudinal extent of the initial methane source is evidently greater in the instantaneous atmosphere emission scenario when compared to the two other emission scenarios after 2 sols, and further evident after 5 sols by which time methane at levels of less than 0.5 ppbv has reached longitudes greater than 180°E in Figure 1i and less than 1 pptv present for the majority of western longitudes in the sustained and instantaneous surface emission scenarios (Figures 1g and 1h, respectively). After 5 sols, differences in the two surface emission scenarios are also becoming apparent, with less than 5 ppbv methane present below 10 km near the initial source longitude in the instantaneous surface emission scenario (Figure 1h), whereas the sustained surface emission scenario in Figure 1g still has methane levels greater than 10 ppbv below 10 km. This suggests that a surface emission of methane will need to be observed for at least 5 sols in order to distinguish if the initial source is sustained or instantaneous (otherwise the sustained surface emission scenario could be potentially incorrectly interpreted as a weaker/stronger instantaneous emission).

Similar peak values of 5–10 ppbv of methane at 10–15 km altitude in all three emission scenarios occur in the vicinity of 0° longitude, with all three different emission scenarios displaying similar vertical profiles at this location. The atmospheric layer formed by the emission scenarios in this study at 2.5°N latitude are at a marginally lower altitude than those simulated by *Viscardy et al.* [2016], potentially as a result of the different latitude of initial emission of methane resulting in weaker ascending motion at the boundary of the ascending branch of the northern and southern Hadley cell.

The different evolutionary behavior of a potential sustained and instantaneous surface emission scenario of methane (beginning to be distinguishable after around 5 sols) is more obvious after 10 sols (Figures 1j and 1k, respectively). While an instantaneous surface emission scenario with a plausible release rate is relatively well mixed at levels of up to 5 ppbv after 10 sols, the sustained surface release scenario now has its greatest methane abundance of more than 100 ppbv near the source location. Methane levels eastward of the initial source longitude at altitudes higher than 20 km are, however, still rather similar. Ten sols after the initial instantaneous release of methane, the instantaneous surface emission scenario and instantaneous atmosphere emission scenario (displayed in Figures 1k and 1l, respectively) are practically identical for the majority of the domain displayed, with differences primarily less than 1 ppbv. This suggests that to determine the initial altitude of the methane source requires observing a release of methane within the first 10 sols, otherwise determining the altitudinal origin of methane will be impossible.

The analysis so far has only investigated a meridional cross section of the methane vertical profile that contains the initial source latitude, but are differences apparent between the three different emission scenarios away from the initial source latitude? Figure 2 displays the evolution of the methane volume mixing ratio vertical profile at a latitude of 27.5°S for the three different emission scenarios. While little difference is evident after 1 sol between the three different emission scenarios, the instantaneous atmosphere emission scenario displayed in Figure 2c shows a peak of around 10 pptv methane at 20 km altitude. This results from stronger meridional transport of methane at higher altitudes coupled with the initial higher altitude of methane in the instantaneous atmosphere emission scenario, with a local maximum of methane greater than 5 ppbv at 10 km slightly west of the initial source longitude in Figure 2f after 2 sols.

After 5 sols, methane levels of up to 5 ppbv are present from 60 to 180°E in the instantaneous atmosphere emission scenario (Figure 2i) and methane levels are up to 2 orders of magnitude lower in the same region for the sustained and instantaneous surface emission scenarios (displayed in Figures 2g and 2h, respectively). Westward of the initial source longitude, the methane vertical profile is similar in all three different emission scenarios, with a peak in methane generally centered at around 10–12 km. The lack of methane below 5 km in all emission scenarios indicates that it would be difficult to know whether the sustained and instantaneous surface emission scenarios originated from a surface emission unless you have observed the methane plume much closer in latitude to the actual source location.

The methane vertical profile at 27.5°S latitude for the sustained and instantaneous surface emission scenarios are almost identical after 5 sols but begin to diverge from one another after 10 sols (see Figures 2j and 2k), with consistent levels of up to 5 ppbv methane present for the majority of the atmosphere below 20 km in the sustained surface emission scenario. The timescale for divergence of a sustained and instantaneous surface emission scenario is similar to when looking at the meridional cross section of methane vertical profile

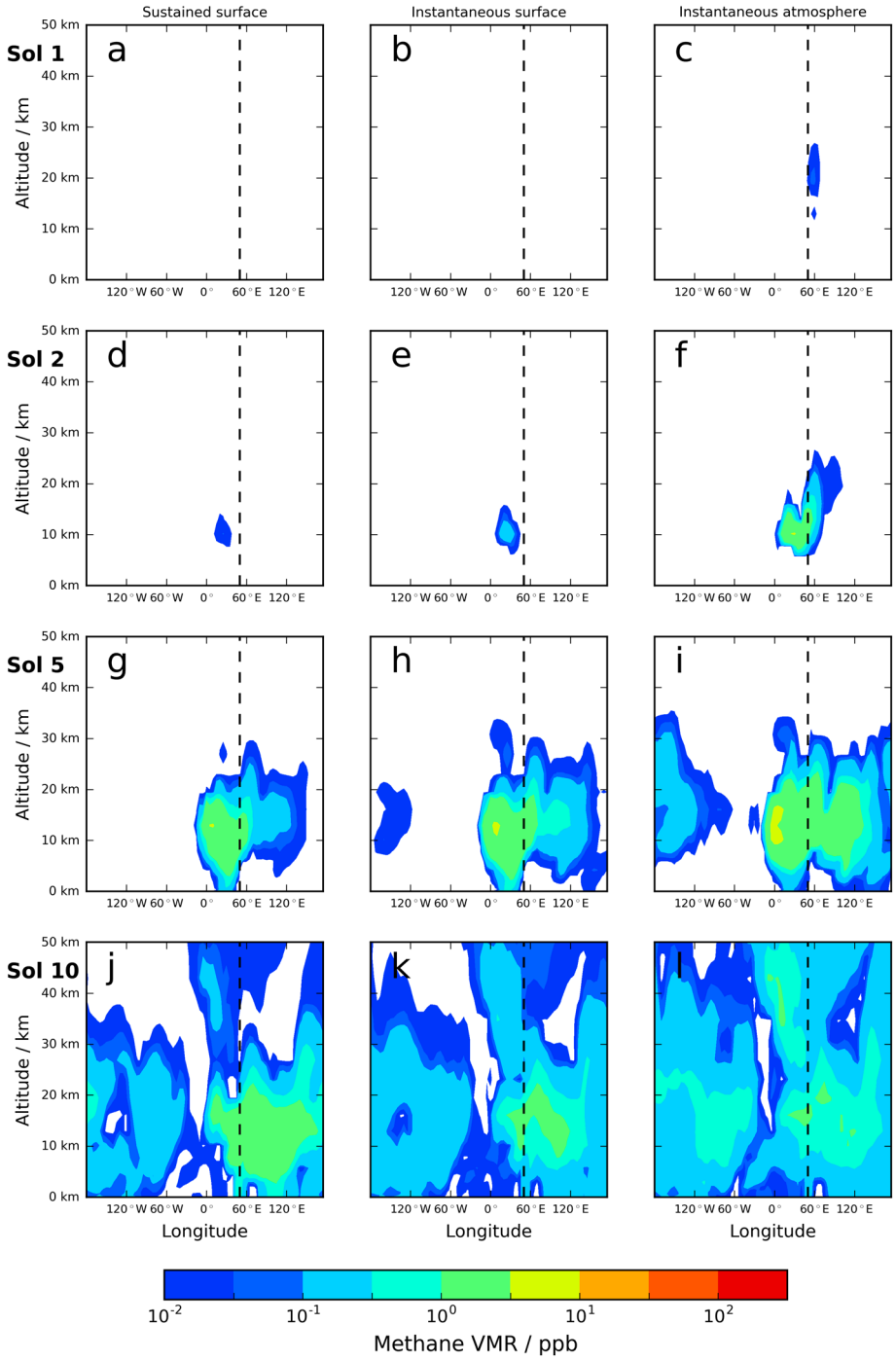


**Figure 2.** Meridional cross section of methane vertical profile at 27.5°S in the sustained surface release scenario (Figures 2a, 2d, 2g, and 2j), instantaneous surface release scenario (Figures 2b, 2e, 2h, and 2k), and instantaneous atmosphere release scenario (Figures 2c, 2f, 2i, and 2l) for the (a–c) first, (d–f) second, (g–i) fifth, and (j–l) tenth sol of simulation. The dashed vertical black line indicates the longitude of the initial source emission (50°E,2.5°N). White indicates methane at levels lower than 10 pptv.

at the source latitude in Figure 1. The continued influx of methane in the sustained surface emission scenario results in methane at an abundance greater than 3 ppbv from 60 to 120°E in Figure 2j, while after 10 sols the instantaneous surface and atmosphere emission scenario are largely well mixed with peak methane abundance of ~1 ppbv (Figures 2k and 2l, respectively). Similar to the meridional cross section of methane vertical profile at the source latitude, 10 sols after the initial emission of methane the instantaneous

surface and atmosphere emission scenarios are almost indistinguishable, with differences generally less than 1 ppbv. Marginally, more methane is present at higher altitudes above 35 km in the instantaneous atmosphere emission scenario (Figure 2l).

For all three different emission scenarios, there is a higher abundance of methane in the vertical profiles at 180–30°W at a latitude of 27.5°S than at the initial source latitude (compare Figures 2j–2l with Figures 1j–1l). Methane is dispersed more extensively in longitude at more southerly latitudes as methane is transported by stronger zonal winds in the southern polar jet at this time of the year.

## 4. Impact of Data Assimilation on Methane Transport and Backtracking

This section looks at the impact on the evolution of a methane plume as a result of the assimilation of TES temperature profiles. Previous studies have indicated how assimilation of thermal data is able to capture the actual transient waves [*Lewis et al.*, 2007] and modify the transient baroclinic wave behavior in a consistent way [*Lewis et al.*, 2016], altering the weather and in particular correcting the amplitude and phase of waves in a GCM. Deviations in the methane distribution as it evolves in time with/without assimilation of temperature profiles are equivalent to deviations in the thermal structure of the atmosphere (since methane is a passive tracer). As the backtracking of methane to its source depends primarily on the circulation patterns and hence thermal structure of the atmosphere, any deviations indicated as the methane plume evolves forward in time with/without assimilation will equivalently translate to inaccuracies in locating spatially the initial source when using a modeling approach to retrace the evolved methane distribution back in time.

The above point is illustrated in Figure 3, which displays the evolution of methane for the instantaneous surface emission scenario without the assimilation of TES temperature profiles. The assimilation of thermal profiles adjusts the local circulation patterns, and after 1 sol the vertical shape of the plume is already different, with a westward tilt evident in the methane plume when no thermal profiles are assimilated (compare Figure 1b with Figure 3a). Differences in the northward/southward transport of methane away from the initial source latitude also contribute to the differences in local methane abundance displayed in Figure 3b. The increased westward transport of methane continues and after 2 sols, methane at an altitude of ~10 km has already formed a distinct atmospheric layer above the equator in Figure 3d, while this feature is only apparent later when the thermal profiles are assimilated (Figure 1h). The dipole in deviation of local methane abundance close to the initial source location below 10 km, i.e., generally more/less methane eastward/westward when thermal profiles are not assimilated in Figure 3e indicates that very different vertical profiles would be retrieved over the initial source location. As the time from the initial emission increases, the observed deviation between methane abundance in the instantaneous surface emission scenario with/without assimilation of thermal profiles extends in longitude. After 10 sols (compare Figure 1k and Figure 3j), peak differences in local methane abundance are around 1 ppbv, which corresponds to as much as a 50% difference in local methane abundance at any point in the domain (Figure 3k), and differences are apparent across almost all longitudes.

Regarding the potential backtracking of a methane source to its initial location, one of the primary science goals of the ExoMars TGO mission, it is important to investigate the direct impact of data assimilation on the evolving wind fields. A primary source of error in the accuracy of backtracking will be in the zonal wind deviations (which in the lower atmosphere are generally larger in magnitude than meridional winds) between the simulation with/without assimilation of thermal profiles. As a result of the regional variability of the surface of Mars [*Ehlmann and Edwards*, 2014], an accurate backtracking of methane is key to provide evidence of the most likely origin of the methane source. Figures 3c, 3f, 3i, and 3l display the zonal wind speed deviation at 2.5°N of the simulation without assimilation after 1, 2, 5, and 10 sols, respectively (averaged over the preceding sol) from the simulation that includes assimilation of TES temperature profiles. Changes in the zonal wind reflect the modifications to the thermal structure of the atmosphere through the assimilation process. The assimilation of thermal profiles results in a strengthening of the easterly zonal winds east of the initial source location above 10 km. The difference in zonal wind speed at the altitude of the atmospheric layer formed (between 10 and 20 km) is in the range of 5–10 $ms^{-1}$ eastward of the initial source longitude (see Figures 3i and 3l), which if consistent over sols 5 to 10 of the evolution of the methane source equates to a difference of 35–70° in longitude. This potential inaccuracy in locating the initial source longitude in the 10–15 km altitude range is (in this specific case study) mitigated by the negative zonal wind speed difference of a similar

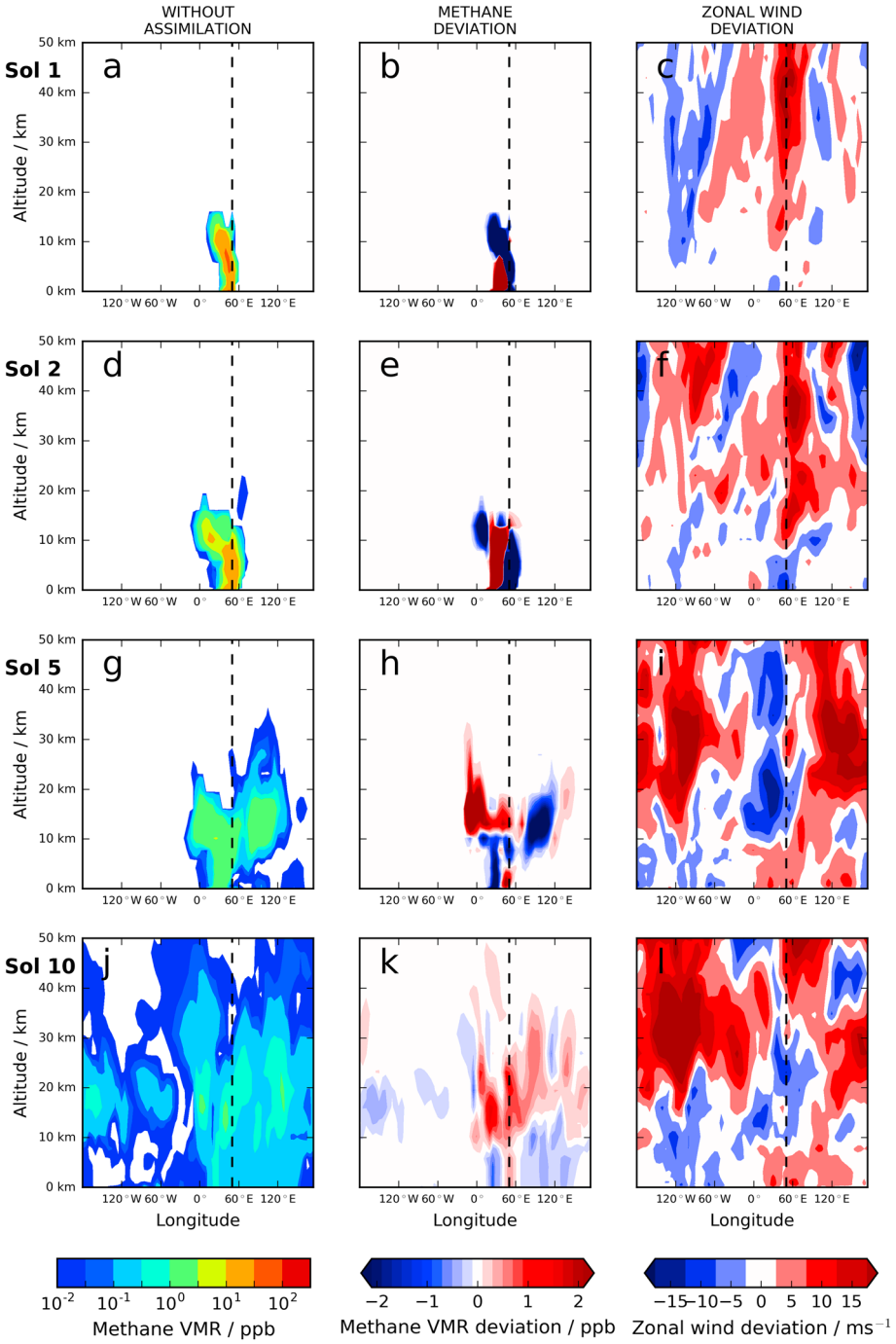


**Figure 3.** Meridional cross section of methane vertical profile at 2.5°N in the instantaneous surface release scenario with no assimilation (Figures 3a, 3d, 3g, and 3j), the methane deviation from the instantaneous surface release scenario (Figures 3b, 3e, 3h, and 3k), and the zonal wind deviation from the instantaneous surface release scenario (Figures 3c, 3f, 3i, and 3l) for the (a–c) first, (d–f) second, (g–i) fifth, and (j–l) tenth sol of simulation. The dashed vertical black line indicates the longitude of the initial source emission (50°E, 2.5°N). White in the left column indicates methane at levels lower than 10 pptv. Zonal wind deviations are averaged over the sol preceding the sol displayed in each row.

magnitude west of the initial source longitude, but methane which is present at marginally higher altitudes (i.e., just above 20 km altitude) will show a large difference in the initial source longitude since the deviation is generally positive over the majority of longitudinal space.

## 5. Conclusions

Analysis of the vertical evolution of methane for three different methane emission scenarios has been performed to determine if it is possible to distinguish between the evolution of different methane release scenarios. This is of high importance for the contextual interpretation of retrievals of the methane vertical profile, possible in the future from the NOMAD and ACS instruments on the ExoMars TGO spacecraft, to determine the original emission location of atmospheric methane.

Using release rates of methane constrained by previous modeling studies and the spatial location of an observed methane plume [*Mumma et al.*, 2009], a comparison was made between a sustained and instantaneous surface release of methane. Distinguishing between a sustained and instantaneous surface emission requires at least 10 sols of tracking the emission (otherwise a continuously emitting methane source could potentially be interpreted incorrectly as a weaker instantaneous emission).

To determine if a methane source is atmospheric rather than from the surface, which can help to identify the underlying release mechanism of methane into the atmosphere, the source of methane must be observed within 10 sols of the initial release. After this timescale, the methane vertical profile for a surface or atmospheric release are practically indistinguishable from one another. An atmospheric source of methane is spread faster in latitudinal space, and so comparison of retrievals of the methane vertical profile spaced up to 30° apart in latitude can give clues to the initial altitude of the methane source, as long as the atmosphere is observed on the timescale covering less than ~5 sols after the initial methane source emission.

The longitudinal distribution of an evolving methane plume depends strongly on an accurate representation of the thermal state of the atmosphere during the evolution of the plume to capture the most realistic circulation patterns. Although the magnitude of deviations will be model dependent, assimilation of thermal profiles from available data will be critical to provide the best estimate of the thermal state of the atmosphere which includes weather and large-scale wave activity. Accurate backtracking of a methane plume to its source location can only be performed using assimilation of both methane vertical profiles and thermal profiles into a GCM, which will be possible using data from instruments on the ExoMars TGO spacecraft in the future.

**Acknowledgments**
The authors gratefully acknowledge the support of the UK Space Agency/STFC. J.A.H. and S.R.L. thank UKSA for support under grant ST/I003096/1, S.R.L. also thanks STFC grant ST/L000776/1, and M.R.P. thanks UKSA for support under grants ST/I003061/1 and ST/P001262/1. All authors acknowledge support as part of the project UPWARDS-633127, funded by the European Union Horizon 2020 Programme. We are grateful for an ongoing collaboration with François Forget and coworkers at LMD and Franck Lefèvre at LATMOS. The model output used in this paper is available by request from the authors.

## References

Atreya, S. K., P. R. Mahaffy, and A.-S. Wong (2007), Methane and related trace species on Mars: Origin, loss, implications for life, and habitability, *Planet. Space Sci.*, *55*, 358–369.

Chassefière, E. (2009), Metastable methane clathrate particles as a source of methane to the Martian atmosphere, *Icarus*, *204*, 137–144, doi:10.1016/j.icarus.2009.06.016.

Colaïtis, A., A. Spiga, F. Hourdin, C. Rio, F. Forget, and E. Millour (2013), A thermal plume model for the Martian convective boundary layer, *J. Geophys. Res. Planets*, *118*, 1468–1487, doi:10.1002/jgre.20104.

Conrath, B. J., J. C. Pearl, M. D. Smith, W. C. Maguire, P. R. Christensen, S. Dason, and M. S. Kaelberer (2000), Mars Global Surveyor Thermal Emission Spectrometer (TES) observations: Atmospheric temperatures during aerobraking and science phasing, *J. Geophys. Res.*, *105*, 9509–9520, doi:10.1029/1999JE001095.

Ehlmann, B. L., and C. S. Edwards (2014), Mineralogy of the Martian surface, *Annu. Rev. Earth Pl. Sc.*, *42*, 291–315, doi:10.1146/annurev-earth-060313-055024.

Fonti, S., and G. A. Marzo (2010), Mapping the methane on Mars, *Astron. Astrophys.*, *512*, A51.

Forget, F., F. Hourdin, R. Fournier, C. Hourdin, O. Talagrand, M. Collins, S. R. Lewis, P. L. Read, and J.-P. Huot (1999), Improved general circulation models of the Martian atmosphere from the surface to above 80 km, *J. Geophys. Res.*, *104*, 24,155–24,176.

Geminale, A., V. Formisano, and G. Sindoni (2011), Mapping methane in Martian atmosphere with PFS-MEX data, *Planet. Space Sci.*, *59*, 137–148.

Holmes, J. A., S. R. Lewis, and M. R. Patel (2015), Analysing the consistency of Martian methane observations by investigation of global methane transport, *Icarus*, *257*, 23–32, doi:10.1016/j.icarus.2015.04.027.

Lefèvre, F., and F. Forget (2009), Observed variations of methane on Mars unexplained by known atmospheric chemistry and physics, *Nature*, *460*, 720–723.

Lewis, S. R., P. L. Read, B. J. Conrath, J. C. Pearl, and M. D. Smith (2007), Assimilation of thermal emission spectrometer atmospheric data during the Mars Global Surveyor aerobraking period, *Icarus*, *192*, 327–347.

Lewis, S. R., D. P. Mulholland, P. L. Read, L. Montabone, R. J. Wilson, and M. D. Smith (2016), The solsticial pause on Mars: 1. A planetary wave reanalysis, *Icarus*, *264*, 456–464, doi:10.1016/j.icarus.2015.08.039.

Madeleine, J.-B., F. Forget, E. Millour, L. Montabone, and M. J. Wolff (2011), Revisiting the radiative impact of dust on Mars using the LMD Global Climate Model, *J. Geophys. Res.*, *116*, E11010, doi:10.1029/2011JE003855.

Montabone, L., F. Forget, E. Millour, R. J. Wilson, S. R. Lewis, B. Cantor, D. Kass, A. Kleinboehl, M. Lemmon, M. D. Smith, and M. J. Wolff (2015), Eight-year climatology of dust optical depth on Mars, *Icarus*, *251*, 65–95.

Mumma, M. J., G. L. Villanueva, R. E. Novak, T. Hewagama, B. P. Bonev, M. A. DiSanti, A. M. Mandell, and M. D. Smith (2009), Strong release of methane on Mars in Northern Summer 2003, *Science*, *323*, 1041–1045.

Navarro, T., J.-B. Madeleine, F. Forget, A. Spiga, E. Millour, F. Montmessin, and A. Määttänen (2014), Global climate modeling of the Martian water cycle with improved microphysics and radiatively active water ice clouds, *J. Geophys. Res. Planets*, *119*, 1479–1495, doi:10.1002/2013JE004550.

Newman, C. E., S. R. Lewis, P. L. Read, and F. Forget (2002), Modeling the Martian dust cycle: 1. Representations of dust transport processes, *J. Geophys. Res.*, *107*, 5123, doi:10.1029/2002JE001910.

Oze, C., and M. Sharma (2005), Have olivine, will gas: Serpentinization and the abiogenic production of methane on Mars, *Geophys. Res. Lett.*, *32*, L10203, doi:10.1029/2005GL022691.

Priestley, A. (1993), A quasi-conservative version of the Semi-Lagrangian advection scheme, *Mon. Weather Rev.*, *121*, 621–629.

Steele, L. J., S. R. Lewis, and M. R. Patel (2014), The radiative impact of water ice clouds from a reanalysis of Mars Climate Sounder data, *Geophys. Res. Lett.*, *41*, 4471–4478, doi:10.1002/2014GL060235.

Stevens, A. H., M. R. Patel, and S. R. Lewis (2017), Modelled isotopic fractionation and transient diffusive release of methane from potential subsurface sources on Mars, *Icarus*, *281*, 240–247, doi:10.1016/j.icarus.2016.08.023.

Summers, M. E., B. J. Lieb, E. Chapman, and Y. L. Yung (2002), Atmospheric biomarkers of subsurface life on Mars, *Geophys. Res. Lett.*, *29*, 2171, doi:10.1029/2002GL015377.

Villanueva, G. L., M. J. Mumma, R. E. Novak, Y. L. Radeva, H. U. Käufl, A. Smette, A. Tokunaga, A. Khayat, T. Encrenaz, and P. Hartogh (2013), A sensitive search for organics ($CH_4$, $CH_3OH$, $H_2CO$, $C_2H_6$, $C_2H_2$, $C_2H_4$), hydroperoxyl ($HO_2$), nitrogen compounds ($N_2O$, $NH_3$, HCN) and chlorine species (HCl, $CH_3Cl$) on Mars using ground-based high-resolution infrared spectroscopy, *Icarus*, *223*, 11–27.

Viscardy, S., F. Daerden, and L. Neary (2016), Formation of layers of methane in the atmosphere of Mars after surface release, *Geophys. Res. Lett.*, *43*, 1868–1875, doi:10.1002/2015GL067443.

Webster, C. R., et al. (2015), Mars methane detection and variability at Gale crater, *Science*, *347*, 415–417.